Bioprinting 18 (2020) e00084

Contents lists available at ScienceDirect

Bioprinting

journal homepage: www.elsevier.com/locate/bprint

Microfabricated and multilayered PLGA structure for the development of co-cultured *in vitro* liver models

Carmelo De Maria, Gabriele Maria Fortunato *, Irene Chiesa, Giovanni Vozzi

Research Centre 'E. Piaggio' and Dept. of Ingegneria dell'Informazione of University of Pisa, Pisa, Italy

ARTICLE INFO

Keywords:
In vitro liver model
Soft lithography
Poly(lactic-co-glycolic acid)
Hepatocytes
Fibroblasts

ABSTRACT

One of the main advantages of having an *in vitro* model is the possibility of reducing toxic effects of drugs on human body and evaluate their response to pharmacological treatments to improve the efficacy of a patient-specific therapy. The limitation of such *in vitro* model is the use of monolayer hepatocytes cultures that show some problems of protein secretion and hepatic functionality. In order to overcome these drawbacks, we present two innovative multilayer structures based on micro-stamped poly(lactic-co-glycolic acid) (PLGA) structures and hepatocytes and fibroblast co-cultures. In particular, the first model consisted of 1 up to 5 layers of PLGA seeded with the previously cited co-culture, while the second model consisted of various sandwich structures of PLGA functionalised (or not) with collagen and seeded with hepatocytes and/or fibroblasts. A mechanical analysis, contact angle and surface charge density measurements were carried out. After these preliminary tests, a metabolic analysis was performed evaluating glucose consumption and urea and albumin production over a culture period of 11 days. Results showed promising application of these *in vitro* liver models, in particular considering the field of cirrhotic liver treatment.

1. Introduction

Liver is a key organ in human-drugs interactions, serving as metabolic hub both in physiological and pathological situations [1]. Liver performs several complex functions that are critical for organism homeostasis, such as the maintenance of blood glucose levels via synthesis and storage of glucose, the secretion of fundamental proteins (e.g.: albumin, transferrin and lipoproteins), the detoxification and excretion of waste products (e.g.: bilirubin and urea) [2–5]. However, liver most important function is metabolism of drugs and xenobiotics.

Therefore, liver response to external molecules is paramount to evaluate early drug-induced toxicity of new potential drugs, with particular attention to metabolic studies and pharmacokinetic property assessment.

In this scenario, *in vitro* models can be used to study pharmacokinetics and hepatoxicity of new drugs in an early stage. *In vitro* models can provide a fine microscopic control of cellular environment and dynamics, as well as isolate cell-based mechanism of action and pathways, reducing the number of animal experiments, and providing a faster and cheaper way for analysis [1,6].

The main goal of an *in vitro* model in liver tissue engineering (LTE) is to identify drug pharmacokinetic, and to predict the potential hepatotoxic effects and unsuitable properties of new drug candidates in order to facilitate their development and improve their quality.

In the past decades, two-dimensional (2D) culture of hepatocytes, that were isolated from rat or human, have been increasingly used as models for LTE. However, their use is limited because hepatocytes dedifferentiate and lose most of their biochemical functions, such as protein synthesis on bile production, over time when they are isolated from their native environment [1,7]. In addition, 2D hepatocytes cultures are characterized by the retainment of cell membrane integrity and a limited life span [8–10].

Several strategies have been developed to overcome these drawbacks, including sandwich configuration (as in this work), three dimensional (3D) spheroids and microfluidic systems, which simultaneously resemble both the structure and the functions of the parental tissue in a closer way than conventional monolayer cultures [11,12].

Treyer et al. [13] developed a sandwich *in vitro* liver model overlaying 2D cultures of hepatocytes with a thin layer of extracellular matrix (ECM) proteins. This system mimics the physiological microenvironment of hepatocytes in vivo, and improves hepatocytes polarization, stabilizing cellular phenotype.

* Corresponding author.
E-mail addresses: carmelo.demaria@unipi.it (C. De Maria), gabrielemaria.fortunato@phd.unipi.it (G.M. Fortunato).

https://doi.org/10.1016/j.bprint.2020.e00084
Received 6 October 2019; Received in revised form 21 January 2020; Accepted 4 March 2020

Differently, Bell et al. [14] fabricated easily scalable 3D hepatocytes spheroids by spontaneous self-aggregation. The authors showed that 3D spheroid culture conditions improve the gene expression signatures and phenotypes of hepatocytes.

Generally, 3D spheroids are the most used system for *in vitro* liver model because they maintain many of liver-specific function such as albumin, urea, transferrin and bile secretion and metabolizing capacities [1,11,15]. However, some limitations arise from them, such as the difficulty in scaling the system down to microfluidic applications [1].

To date, the biggest challenge of LTE is still the ability to preserve liver-specific function *in vitro*. In fact, so far, an adequately differentiated hepatic phenotype was maintained for just one week after isolation from a rat liver [16]. Several parameters have been proved to play a role in maintaining hepatic function. Most important ones are the presence of an adequate nutrient supply provided by a multicomponent medium, an extracellular environment rich with ligands for adhesion and signalling, and a spatial architecture resembling the native liver [17].

In our work, we present two different *in vitro* liver models that mimic the multilayer structure of native liver. The first one comprises different biofabricated structures seeded with fibroblasts and hepatocytes. The second one consists of a sandwich structure made up of cells and structures functionalised in different ways. Thus, both models try to recreate the multilayer structure typical of native liver to enhance hepatocytes functionality and create the proper environment for hepatocytes development. The presented work is a very preliminary study, since it is based on a 7-days cell culture period. Nevertheless, it showed promising results for the application in LTE and there will be further investigation on the down-scalability and long-term stability of the model.

2. Materials and methods

2.1. Polymer solution

A poly(lactic-co-glycolic acid) (PLGA) solution was obtained by dissolving 85/15 PLGA (Lactel absorbable polymers, USA, MW 18,000) in chloroform to have a 20% (w/v) concentration. This solution was used for the scaffold fabrication.

2.2. Sample preparation

Silicon 100 wafers were spin-coated with EPON-SU8 photoresist (Microchem Co., Newton, MA, USA), baked to drive away the solvent, and then exposed to UV light in a Bottom Side Mask Aligner (Karl Suss, Waterbury Center, VT) through a mask. The mask was created using CorelDraw and printed on a transparency using a commercial high-resolution line printer. Exposed photoresist was then developed (SU8 developer, Microchem Co.) and subsequently the wafers were baked. PDMS prepolymer was prepared by mixing the commercially available prepolymer and catalyser (Sylgard 184 kit, Dow Corning) in a 10:1 w/w ratio. The PDMS mould was casted from a microfabricated silicon master. The mixture was degassed under vacuum to eliminate bubbles created during mixing. The pre-polymer solution was casted on the master and placed under vacuum once again to remove any bubbles that may have been introduced. PDMS was cured by baking for 2 h at 65 °C. After cooling to room temperature, the PDMS was peeled from the silicon master. The mould was then washed with 70% ethanol and sonicated for 5 min prior to use.

The PLGA solution was deposited on the PDMS mould and placed under vacuum for 2min. During this time the polymer filled the microchannels present in the mould and displaced any air present [18–20]. Once the polymer had filled the mould, excess PLGA was removed by dragging the edge of a glass slide across the top of the mould. The filled mould was baked for 30 min at 60 °C. When cooled, the PLGA pattern was easily removed with a pair of tweezers. The topology of realised structure was a 2D layer with square holes of 300 μm side spaced of 400 μm, as shown in Fig. 1.

2.3. Mechanical characterization

Mechanical characterization was carried out performing uniaxial tensile tests using a uniaxial testing machine Zwick-Roell Z005 ProLine equipped with a 100 N load cell [21,22]. Two different samples were tested. The first one was a PLGA casted film, while the second was the grid structure prepared as described in the previous section. These different structures were compared to highlight different mechanical properties due to the geometry of specimen. Samples were pulled with a strain rate of 10%/min of the initial length until failure. Stress-strain curves were obtained for each sample, and elastic modulus was evaluated as the initial slope of the stress-strain curve.

2.4. Contact angle

Static contact angle was measured using the sessile drop method, with a 5 μl double distilled water droplet at room temperature. Images were acquired with a horizontal optical microscope equipped with a digital camera and the CAM 200 software. The test was performed on dried samples; for each angle reported, at least five measurements on different surface locations were averaged. Wettability was determined as crucial for cell adhesion and proliferation: cells adhere onto polymer surfaces presenting moderate wettability (water contact angles of 40–80°) [23–25].

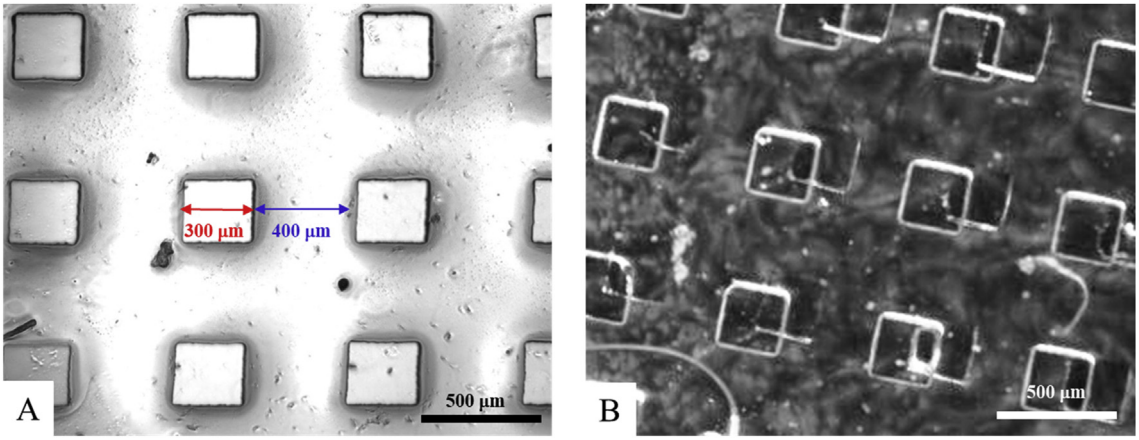

Fig. 1. A) PLGA single layer structure with square holes of 300 μm side spaced of 400 μm – B) Two layers PLGA structure.

2.5. Surface charge density

Surface potential measurements were made using a Kelvin vibrating plate (KSV Instruments, Sweden), with a nominal error of ± 10 mV [26]. The Kelvin vibrating plate measures the surface potential between two conductors, the sample holder and probe respectively, placed about 1 mm apart. The difference in measured potential between the sample holder with and without (reference potential) the sample is given by the surface potential of the sample, and it depends on its thickness, dielectric constant and surface charge density. Three samples were analyzed. After the acquisition of the reference potential (i.e. sample holder without sample), the thickness of sample and the distance between the specimen and the vibrating plate were measured. The potential difference was evaluated every 10 min using a purposely written software, developed in Matlab®. Data were filtered with a moving average filter and the variance analysis was performed in order to determine when the signal presented a constant trend, which was taken to evaluate the surface charge density of polymer. The grid pattern of PLGA samples was schematized as a parallel of a capacitor representing air and a series of two capacitors representing PLGA and air respectively, as shown in Fig. 2.

Calculations to evaluate surface charge density σ are shown in equations 1 and 2 (C: capacitance; Q = charge; V = electric potential; e_0/e_r: vacuum/relative permittivity; A: area; d: distance between plates).

$$C_{TOT} = C_{A2} + \frac{C_{A1}C_P}{C_{A1}+C_P} = \frac{\varepsilon_0 A}{2d} + \left[\frac{\frac{\varepsilon_0 A}{d}\frac{\varepsilon_0\varepsilon_r A}{d}}{\frac{\varepsilon_0 A}{d}+\frac{\varepsilon_0\varepsilon_r A}{d}}\right] = \frac{\varepsilon_0 A}{d}\left[\frac{1}{2}+\frac{\varepsilon_r}{\varepsilon_r+1}\right] = \frac{Q}{V} \quad (1)$$

$$\sigma = \frac{Q}{A} = \frac{C_{TOT}V}{A} = \frac{\varepsilon_0}{d}\left[\frac{1}{2}+\frac{\varepsilon_r}{\varepsilon_r+1}\right]V \quad (2)$$

The aim of this test was to determine the surface potential or charge that can have influence on cell adhesion [27,28].

2.6. Cell cultures

Rat hepatocytes were isolated from 2- to 3-months old female Lewis rats (Charles River, USA) by collagenase perfusion [29–31]. Briefly, animals were anesthetized, and the portal vein was cannulated. The liver was then perfused with buffers and digested with collagenase. The resultant digest was purified using centrifugation. Hepatocytes were cultured in Dulbecco's Modified Eagle Medium (DMEM) with high glucose (Sigma-Aldrich, Italy), 10% (v/v) foetal bovine serum (Sigma-Aldrich, Italy), 0.5 U/ml insulin (Sigma-Aldrich, Italy), 7 ng/ml glucagon (Sigma-Aldrich, Italy), 7.5 μg/ml hydrocortisone (Sigma-Aldrich), and 1% penicillin-streptomycin (Sigma-Aldrich, Italy). J2-3T3 fibroblasts were cultured in DMEM with high glucose, 10% bovine serum, and 1% penicillin–streptomycin.

Hepatocytes and Fibroblasts were seeded (5 × 10⁵ cells/cm2) in the well or on scaffolds using 2 ml of complete medium per well in ratio 1:1. After 24 h, the polymeric structures were moved to a new micro-well plate to eliminate interference from non-adherent cells. Fibroblasts in co-culture help to modulate function and viability of rat hepatocytes thus avoiding their short-term survival and rapid de-differentiation.

Before seeding, scaffolds and films were placed in a desiccator under vacuum for at least 1 week, and then washed extensively with deionised water and dried in an oven at 50 °C. Following this, the structures were placed in 24-well plates (Sarstedt, Verona, Italy) and sterilised using a standard hospital H2O2 Gas-Plasma protocol available at our clinical facilities. To promote cell attachment, 5 μg/cm2 purified collagen, PureColTM (INAMED, Leimuiden, The Netherlands), was pipetted over the structures and after 1h incubation at 37 °C, they were washed with PBS three times and equilibrated with fresh medium overnight in the incubator.

Both scaffolds and films were coated with an alginate film consisting of 250 μL 1% sodium alginate dissolved in serum-free medium, cross-linked with 50 μl 1% CaCl2 (both from Sigma-Aldrich, Milan, Italy). Excess alginate was removed with a pipette. The resulting film had a thickness of a few tens of microns as measured by an optical profilometer (Opto NCDT, model ILD1400-10, UK), having a nominal resolution of 1 μm. The profilometer uses a small laser spot (0.7 mm × 0.5 mm) which is reflected off a surface. Displacements were calibrated using an uncoated glass slide as a reference. The coating was not uniform and flat as observed by an optical microscope, and this was also reflected in the scatter of the profilometer readings across the slide (40–100 μm). At the low alginate concentrations used, the diffusion coefficient of oxygen and of small solutes is similar to that in water [32–35].

Finally, 2 ml fresh medium were added to each well to begin the experiment. Cells were maintained on the structures for a week and cell counting and medium collection was performed daily. The experiment was performed in triplicate using 21 structures, three samples were sacrificed for counting per day, and the culture medium was changed every two days.

2.7. In vitro testing

Two different types of experiments were performed.

In the first experiment the micro-stamped PLGA layer was seeded with a co-culture of Hepatocytes and fibroblasts in 1:1 ratio as reported in the previous paragraph and after 24 h they were moved to a new micro-well plate to eliminate interference from non-adherent cells and they were stacked up until having 5 different structures composed of 1–5 layers. In the second, a sandwich of cells and structures, as reported in Table 1, was fabricated.

This experiment was performed for 11 days and each two days cell culture media was removed and collected for metabolic analysis and changed in the multiwell.

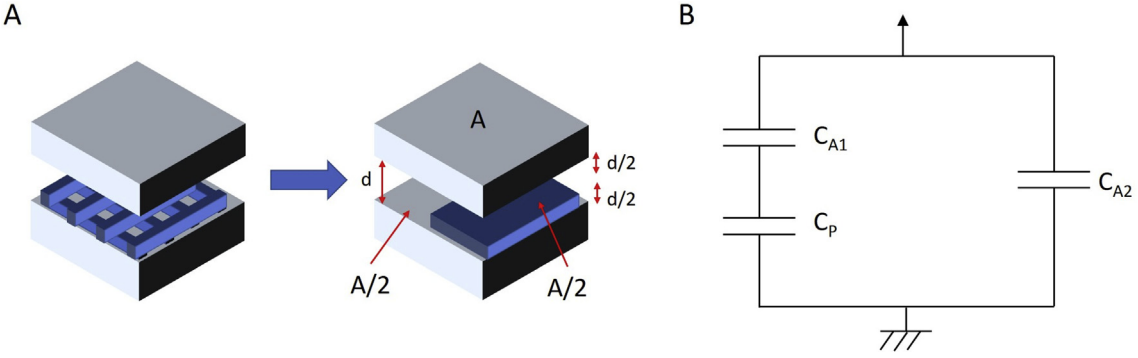

Fig. 2. Model of surface charge density measurement setup (A) and related circuit model (B). (C_P: PLGA capacitance; C_A: air capacitance; A: area; d: distance between plates; blue material represents PLGA).

Table 1
Different experiments carried out changing structure layers and cells.

Structure	Composition
1	Micro-stamped PLGA layer seeded with Hepatocytes
2	Micro-stamped PLGA layer functionalised with collagen and seeded with Hepatocytes
3	Micro-stamped PLGA layer seeded with Hepatocytes covered by micro-stamped PLGA layer seeded with Hepatocytes
4	Micro-stamped PLGA layer seeded with Hepatocytes covered by micro-stamped PLGA layer seeded with fibroblasts
5	Micro-stamped PLGA layer functionalised with collagen and seeded with Hepatocytes and covered by another micro-stamped PLGA layer seeded with Hepatocytes
6	Micro-stamped PLGA layer functionalised with collagen and seeded with Hepatocytes and covered by another micro-stamped PLGA layer seeded with Fibroblasts
7	Micro-stamped PLGA layer functionalised with collagen and seeded with Hepatocytes and covered by another micro-stamped PLGA layer functionalised by collagen and seeded with fibroblasts

2.8. *In vitro assays to assess hepatic function*

Albumin production, which characterises the specific functional activity of liver cells [34], was measured by an enzyme-linked immunosorbent assay (ELISA) (Bethyl Laboratories, Montgomery, TX, USA). A standard curve was made using purified human albumin under the conditions recommended by the manufacturer. Species specificity of the anti-human albumin antibodies was verified using foetal bovine serum (FBS). Glucose consumption and urea production were quantified using commercial enzymatic kits according to the manufacturers' instructions (Megazyme International Poncarale, Italy, and Urea Kit, Sigma-Aldrich, respectively). To compare data from different experiments with different cell numbers and media volumes, glucose, albumin and urea data were expressed as quantities consumed or produced per cell per day, and therefore as rates, not cumulative quantities.

2.9. *Statistical analysis*

Data are expressed as the mean ± standard error. Statistical significance was determined using one-way ANOVA test.

3. Results

3.1. *Physical characterization*

Mechanical properties were investigated on three different PLGA samples, both on grid and film structures. An example of stress-strain curve is showed in Fig. 3.

PLGA grids showed a Young' Modulus of 6.53 ± 0.50 MPa, while films resulted more rigid with a 42.77 ± 1.23 MPa elastic modulus. Grids resulted also more stretchable with a strain at break up to 30%, showing mechanical properties closer to that of soft tissues; however, these mechanical properties should be tuned in further experiments (*e.g.* reducing stiffness) to better mimic liver tissue. A possible solution to this drawback could be playing on the grid pattern to reduce the stiffness of the PLGA matrix.

Contact angle measurement highlighted an acceptable hydrophilicity with an angle $\alpha = (78.2 \pm 3.4)^{\circ}$. This value allows good cell interaction and adhesion.

From the model presented above, the surface charge density resulted $\sigma = 4.42 \pm 0.04$ nC/m2. It is well known that cells, due to the nature of the cytoplasmic lipid membrane, present a small negative external electrical charge. Because of this reason, they make a continuous contact with positively charged substrates, whereas in general, they present only discontinuous focal contacts with negatively charged substrates. Interaction with positive surfaces, as PLGA samples of the presented study, are thus favored.

3.2. *In vitro assays to assess hepatic function*

Results of cell culture on different structure are shown in Figs. 4 and 5, respectively for the first and the second type of experiment.

Glucose consumption, urea production and albumin release for two different experiments are reported in Fig. 5. Multilayer structures (first type of experiment) have the same behavior (no statistical differences; p-value > 0.05) regardless of the number of layers (Fig. 6A-C-E). Glucose consumption reaches a plateau around day 7 of culture, whereas urea and albumin tends to decrease during the 11-days culture period. The same trend was also found for 7 different structures tested during the second experiment (Fig. 6B-D-F). There are no statistical significant differences among different structures (p-value > 0.1).

One-way ANOVA also showed that two datasets (first and second experiment) are statistically not different (p-value > 0.1) thus making both experiments promising for the realization of *in vitro* liver models.

4. Discussion

In this work we presented two different experiments towards the realization and validation of an *in vitro* liver model. Both tests showed similar outcomes thus resulting equally promising for the realization of a liver model. In particular, to assess liver functionality, glucose consumption and urea and albumin production were monitored. Hepatocyte cultures, generally, show loss of biochemical function, such as reduction of protein synthesis. This behavior is mainly due to the hepatocyte adaptation to the culture conditions and the withdrawal from their natural environment. Specifically, urea and albumin secretion are indicators for long-term functional performance of hepatocytes [5]. Albumin was

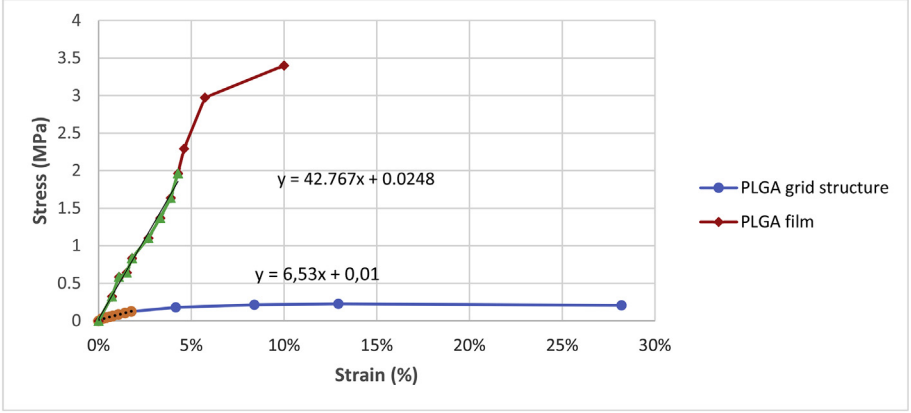

Fig. 3. Stress-strain curve of a two different PLGA samples (grid structure and film) obtained by soft-lithography.

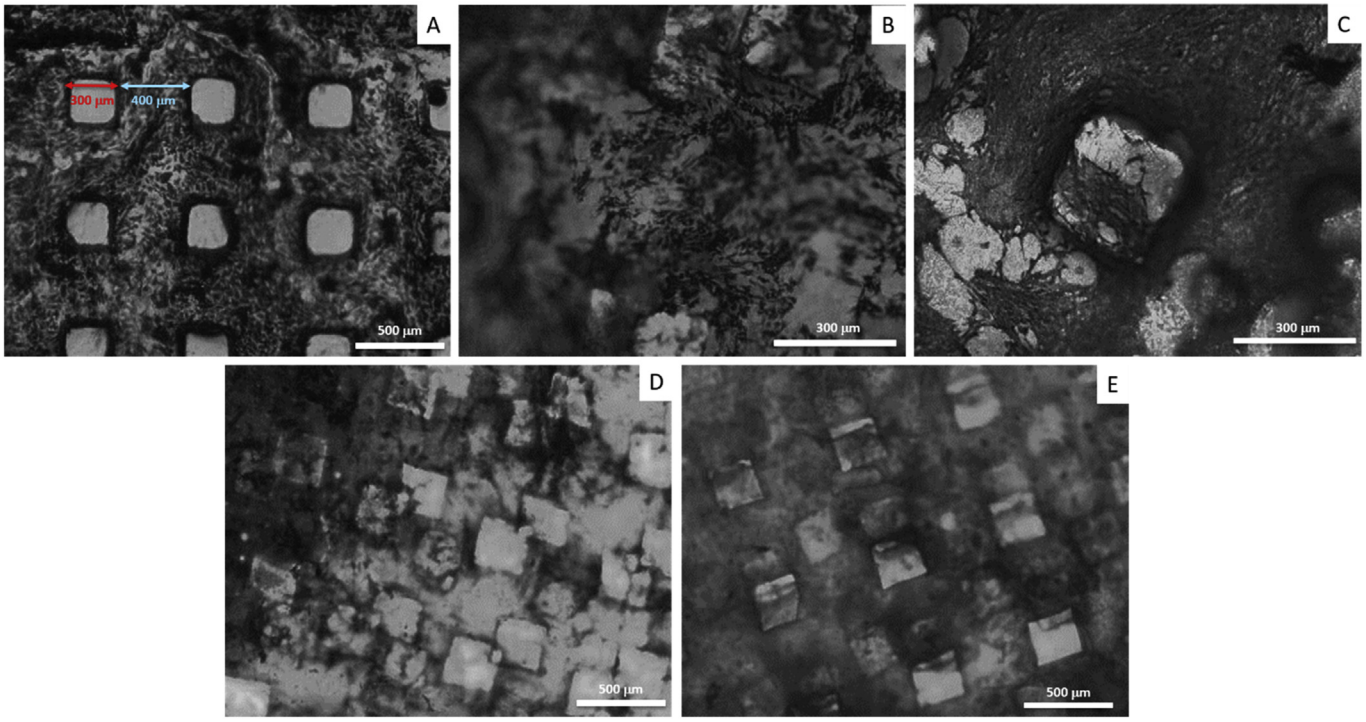

Fig. 4. Structures composed of different layers number of micro-stamped PLGA seeded with a co-culture of hepatocytes and fibroblasts 1:1: A) 1 layer - B) 2 layers - C) 3 layers - D) 4 layers - E) 5 layers. Geometrical properties of the grid structure are highlighted in A.

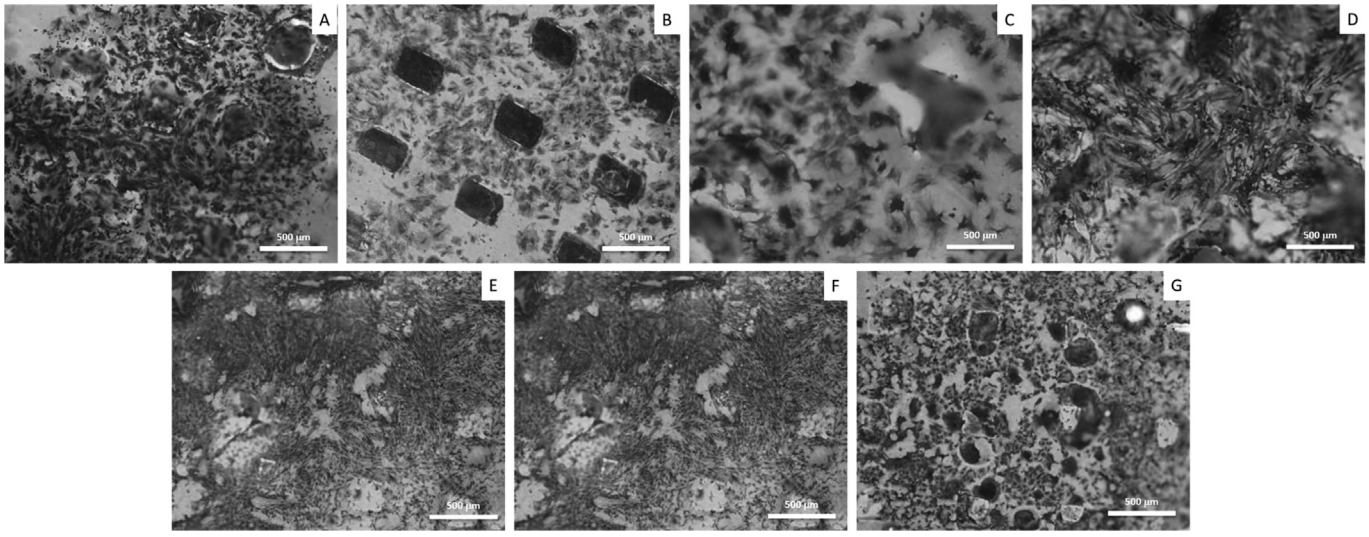

Fig. 5. Different structures realised: A) PLGA + hepatocytes - B) PLGA + collagen + hepatocytes - C) PLGA + hepatocytes + PLGA + hepatocytes - D) PLGA + hepatocytes + PLGA + fibroblasts - E) PLGA + collagen + hepatocytes + PLGA + hepatocytes - F) PLGA + collagen + hepatocytes + PLGA + fibroblast - G) PLGA + collagen + hepatocytes + PLGA + collagen + fibroblasts.

measured as the main protein synthesized specifically by hepatocytes [34]. The glucose metabolism in human hepatocytes *in vivo* is a complex and strictly regulated process. Hepatocyte sources, culture microenvironment and media composition severely alter the glucose metabolism of hepatocytes *in vitro*. In this work glucose consumption is described for each experiment. As can be seen from reported graphs, glucose consumption increases during the 11 days culture period meaning that cells are not releasing glucose, but fibroblast contribute to its consumption. Increasing the number of hepatocytes and fibroblasts layers, glucose consumption is higher due to a larger number of cells. Albumin and urea production, instead, shows a decreasing trend during 11 days. This behavior can be explained considering that albumin is degraded by fibroblasts. The total amount of albumin produced is in fact decreasing with an increase of the number of layers [36]. An interesting application of the developed *in vitro* liver model could be the investigation of cirrhosis treatment. In fact, parameters found from our experiments showed a metabolic trend similar to that of patients with advanced cirrhosis. Normal albumin concentration in healthy conditions should be around 3–5 g/dl, much higher than values found in our work (max value found is 1.6 pg/cell corresponding to 40 mg/dl). Cirrhotic patients, in fact, almost always have hypoalbuminemia caused both by decreased synthesis by the hepatocytes and water and sodium retention that dilutes

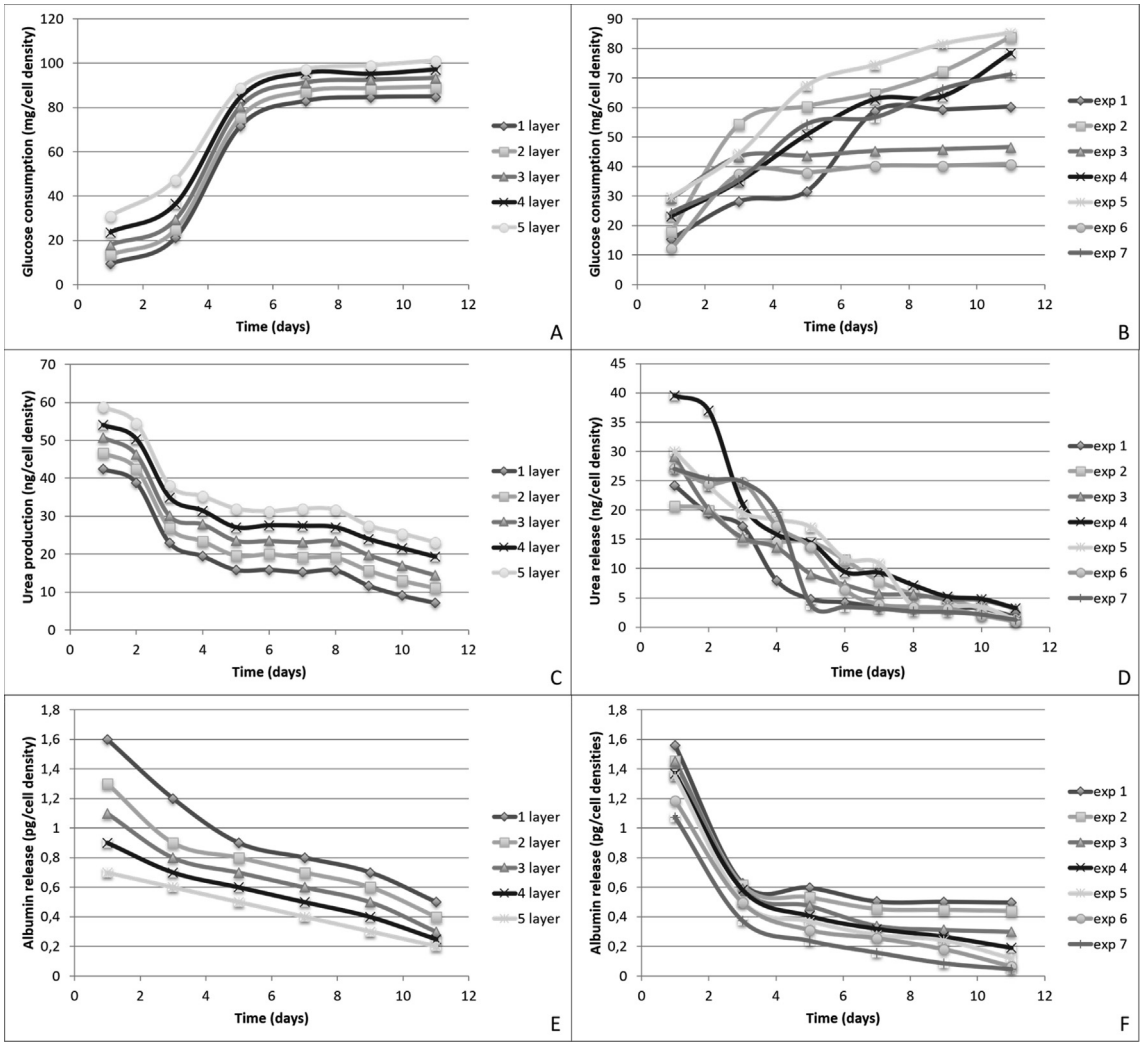

Fig. 6. Glucose consumption: A) Sandwich structures with different number of layers – B) Different structures according to Table 1; **Urea production**: C) Sandwich structures with different number of layers – D) Different structures according to Table 1; **Albumin release**: E) Sandwich structures with different number of layers – F) Different structures according to Table 1.

the content of albumin in the extracellular space. Other factors likely contribute to the development of hypoalbuminemia, including an increased transcapillary transport rate [37–39]. Liver cirrhosis is the end stage of chronic liver disease and is very difficult to treat. Nowadays, liver transplantation is one of the only effective therapies available, even if, serious problems are associated with this technique, such as lack of donors, surgical complications, rejection, and high cost. This *in vitro* model approach could facilitate the investigation of new therapies for the treatment of such disease reducing complications of currently used invasive procedures [40–42].

5. Conclusion

This work presented two promising *in vitro* models of liver based on a multi-layer structure that allowed to avoid the classic problems encountered in monolayer cultures. Results of the metabolic activity of the hepatocyte culture, which are the most significant in the context of this *in vitro* model, showed a behavior similar to that of a cirrhotic liver. On this basis, the proposed model can be further developed for the more in-depth study of liver cirrhosis treatment, in order to obtain a more effective patient-specific therapy and reduce the invasive and often unsuccessful currently used approaches.

Declaration of competing interest

The authors declare that they have no known competing financial interests or personal relationships that could have appeared to influence the work reported in this paper.

CRediT authorship contribution statement

Carmelo De Maria: Writing - original draft, Investigation. **Gabriele Maria Fortunato:** Writing - original draft, Data curation. **Irene Chiesa:** Investigation, Data curation. **Giovanni Vozzi:** Funding acquisition, Supervision.

References

[1] O.B. Usta, et al., Microengineered cell and tissue systems for drug screening and toxicology applications: evolution of in-vitro liver technologies, Technology 3 (1) (2015) 1–26, https://doi.org/10.1142/S2339547815300012.
[2] R. Gebhardt, et al., New hepatocyte in vitro systems for drug metabolism: metabolic capacity and recommendations for application in basic research and drug development, standard operation procedures, Drug Metab. Rev. 35 (2–3) (2003) 145–213, https://doi.org/10.1081/DMR-120023684.
[3] A.K. Nussler, et al., The suitability of hepatocyte culture models to study various aspects of drug metabolism, ALTEX Altern. zu Tierexperimenten 18 (2) (2001) 91–101.

[4] S. Schmitmeier, et al., Development and characterization of a small-scale bioreactor based on a bioartificial hepatic culture model for predictive pharmacological in vitro screenings, Biotechnol. Bioeng. 95 (6) (2006) 1198–1206, https://doi.org/10.1002/bit.21089.
[5] J.P. Miranda, et al., Towards an extended functional hepatocyte in vitro culture, Tissue Eng. C Methods 15 (2) (2009) 157–167, https://doi.org/10.1089/ten.tec.2008.0352.
[6] K. Rehberger, et al., In vitro or not in vitro: a short journey through a long history, Environ. Sci. Eur. 30 (1) (2018), https://doi.org/10.1186/s12302-018-0151-3.
[7] J.C.Y. Dunn, et al., Hepatocytes in collagen sandwich: evidence for transcriptional and translational regulation, J. Cell Biol. 116 (4) (1992) 1043–1053, https://doi.org/10.1083/jcb.116.4.1043.
[8] N. Fausto, et al., Liver regeneration, J. Hepatol. 32 (2000) 19–31.
[9] A.A. Demetriou, et al., Transplantation of microcarrier-attached hepatocytes into 90% partially hepatectomized rats, Hepatology 8 (5) (1988) 1006–1009, https://doi.org/10.1002/hep.1840080505.
[10] H.L. Leffert, et al., Studies on primary cultures of differentiated fetal liver cells, J. Cell Biol. 52 (3) (1972) 559–568, https://doi.org/10.1083/jcb.52.3.559.
[11] C.C. Bell, et al., Comparison of hepatic 2D sandwich cultures and 3d spheroids for long-term toxicity applications: A multicenter study, Toxicol. Sci. 162 (2) (2018) 655–666, https://doi.org/10.1093/toxsci/kfx289.
[12] J.J. Maher, Primary hepatocyte culture: is it home away from home? Hepatology 8 (5) (1988) 1162–1166, https://doi.org/10.1002/hep.1840080534.
[13] A. Treyer, et al., Hepatocyte polarity, Comp. Physiol. 3 (2013) 243–287, https://doi.org/10.1002/cphy.c120009.
[14] C.C. Bell, et al., Characterization of primary human hepatocyte spheroids as a model system for drug-induced liver injury, liver function and disease, Sci. Rep. 6 (25187) (2016) 1–13, https://doi.org/10.1038/srep25187.
[15] V.Y. Soldatow, et al., In vitro models for liver toxicity testing, Toxicol. Res. (Camb). 2 (1) (2013) 23–39, https://doi.org/10.1039/C2TX20051A.
[16] A. Guillouzo, Liver cell models in in vitro toxicology, Environ. Health Perspect. 106 (2) (1998) 511–532, https://doi.org/10.1289/ehp.98106511.
[17] B. Vinci, et al., In vitro liver model using microfabricated scaffolds in a modular bioreactor, Biotechnol. J. 5 (2) (2010) 232–241, https://doi.org/10.1002/biot.200900074.
[18] G. Vozzi, et al., Fabrication of PLGA scaffolds using soft lithography and microsyringe deposition, Biomaterials 24 (14) (2003) 2533–2540, https://doi.org/10.1016/s0142-9612(03)00052-8.
[19] G. Vozzi, et al., Microfabricated PLGA scaffolds: A comparative study for application to tissue engineering, Mater. Sci. Eng. C 20 (1–2) (2002) 43–47.
[20] M. Mattioli-Belmonte, et al., Rapid-prototyped and salt-leached PLGA scaffolds condition cell morpho-functional behavior, J. Biomed. Mater. Res. 85 (2) (2008) 466–476, https://doi.org/10.1002/jbm.a.31483.
[21] Y. Whulanza, et al., Electrical and mechanical characterisation of single wall carbon nanotubes based composites for tissue engineering applications, J. Nanosci. Nanotechnol. 13 (1) (2013) 188–197, https://doi.org/10.1166/jnn.2013.6708.
[22] M. Mariani, et al., Characterization of tissue-engineered scaffolds microfabricated with PAM, Tissue Eng. 12 (3) (2006) 547–557, https://doi.org/10.1089/ten.2006.12.547.
[23] J. Ho Lee, et al., A wettability gradient as a tool to study protein adsorption and cell adhesion on polymer surfaces, J. Biomater. Sci. Polym. Ed. 4 (5) (1993) 467–481, https://doi.org/10.1163/156856293x00131.
[24] Y. Arima, et al., Effect of wettability and surface functional groups on protein adsorption and cell adhesion using well-defined mixed self-assembled monolayers, Biomaterials 28 (20) (2007) 3074–3082, https://doi.org/10.1016/j.biomaterials.2007.03.013.
[25] D.P. Dowling, et al., Effect of surface wettability and topography on the adhesion of osteosarcoma cells on plasma-modified polystyrene, J. Biomater. Appl. 26 (3) (2011) 327–347, https://doi.org/10.1177/0885328210372148.
[26] G.M. Fortunato, et al., Electrospun structures made of a hydrolyzed keratin-based biomaterial for development of in vitro tissue models, Front. Bioeng. Biotechnol. 7 (2019) 1–12, https://doi.org/10.3389/fbioe.2019.00174, no. July.
[27] H.Y. Chang, et al., Effect of surface potential on epithelial cell adhesion, proliferation and morphology, Colloids Surf. B Biointerfaces 141 (2016) 179–186, https://doi.org/10.1016/j.colsurfb.2016.01.049, 1.
[28] H.Y. Chang, et al., Effect of surface potential on NIH3T3 cell Adhesion and proliferation, J. Phys. Chem. 118 (26) (2014) 14464–14470.
[29] J.C.Y. Dunn, et al., Long-term in vitro function of adult hepatocytes in a collagen sandwich configuration, Biotechnol. Prog. 7 (1991) 237–245, https://doi.org/10.1021/bp00009a007.
[30] S. March, et al., Microenvironmental regulation of the sinusoidal endothelial cell phenotype in vitro, Hepatology 50 (3) (2009) 920–928, https://doi.org/10.1002/hep.23085.
[31] P.O. Seglen, Preparation of isolated rat liver cells, Methods Cell Biol. 13 (C) (1976) 29–83.
[32] J. Øyaas, et al., The effective diffusion coefficient and the distribution constant for small molecules in calcium-alginate gel beads, Biotechnol. Bioeng. 47 (4) (1995) 492–500, https://doi.org/10.1002/bit.260470411.
[33] M. Grassi, et al., Experimental determination of the theophylline diffusion coefficient in swollen sodium-alginate membranes, J. Contr. Release 76 (1–2) (2001) 93–105, https://doi.org/10.1016/s0168-3659(01)00424-2.
[34] M. Lübberstedt, et al., HepaRG human hepatic cell line utility as a surrogate for primary human hepatocytes in drug metabolism assessment in vitro, J. Pharmacol. Toxicol. Methods 63 (1) (2011) 59–68, https://doi.org/10.1016/j.vascn.2010.04.013.
[35] A. Venâncio, et al., Characterization of sugar diffusion coefficients in alginate membranes, Biotechnol. Tech. 11 (3) (1997) 183–185.
[36] I. Wagner, et al., A dynamic multi-organ-chip for long-term cultivation and substance testing proven by 3D human liver and skin tissue co-culture, Lab Chip 13 (18) (2013) 3538–3547, https://doi.org/10.1039/c3lc50234a.
[37] M. Bernardi, et al., Human albumin in hte managment of complications of liver cirrhosis, Crit. Care 16 (2) (2012).
[38] S. Walayat, et al., Role of albumin in cirrhosis : from a hospitalist ' s perspective, J. Community Hosp. Intern. Med. Perspect. 7 (1) (2017) 8–14, https://doi.org/10.1080/20009666.2017.1302704.
[39] N. Made, et al., Albumin infusion in liver cirrhotic patients, Acta Med. Indones. 42 (3) (2010) 162–168.
[40] S. Terai, et al., Improved liver function in patients with liver cirrhosis After autologous bone marrow cell infusion therapy, Stem Cell. 24 (10) (2006) 2292–2298, https://doi.org/10.1634/stemcells.2005-0542.
[41] E. Imano, et al., Impaired splanchnic and peripheral glucose uptake in liver cirrhosis, J. Hepatol. 31 (3) (1999) 469–473, https://doi.org/10.1016/s0168-8278(99)80039-7.
[42] T. Nishida, Diagnosis and clinical implications of diabetes in liver cirrhosis: A focus on the oral glucose tolerance test, J. Endocr. Soc. 1 (7) (2017) 886–896, https://doi.org/10.1210/js.2017-00183.